THE JOURNAL OF PHYSICAL CHEMISTRY B

Article

pubs.acs.org/JPCB

Aggregation Features and Fluorescence of Hoechst 33258

Natalia Busto,[†] Beatriz Cano,[†] Rocío Tejido,[†] Tarita Biver,[‡] José M. Leal,[†] Marcella Venturini,[‡] Fernando Secco,[‡] and Begoña García*[,†]

[†]Departamento de Química, Universidad de Burgos, 09001 Burgos, Spain

[‡]Dipartimento di Chimica e Chimica Industriale, Università di Pisa, 56126 Pisa, Italy

ABSTRACT: The functionality of the bisbenzimide Hoechst 33258 in solution has been largely exploited in the quantification of DNA. Understanding of its behavior is essential to promote its widespread application and learning of biological processes. A detailed study of the dimerization process of the fluorescent blue dye Hoechst 33258 is carried out by isothermal titration calorimetry, absorbance, fluorescence, differential scanning calorimetry and T-jump kinetic measurements. The dimer/monomer ratio depends on the dye concentration and the ionic strength. The dimerization constant determined under physiological conditions (pH = 7.0; I = 0.10 M), $K_D = 3 \times 10^4$ M^{-1}, conveys that only micromolar concentrations of the dye can ensure reasonably high amounts of the monomer species in solution. For instance, for 10 μM dye content, the dimer prevails for I > 0.08 M, whereas the monomer is observed at low ionic strength, a key issue to be elucidated as long as the dimer species is more fluorescent than the monomer and the fluorescence intensity strongly relies on the ionic strength and the dye concentration.

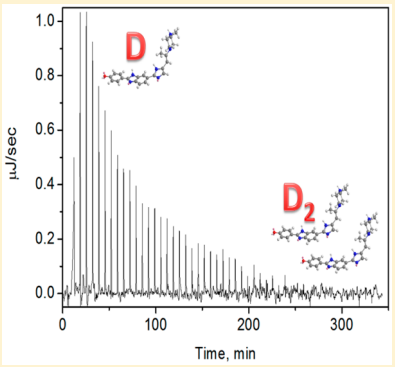

INTRODUCTION

Hoechst 33258 is a bisbenzimide widely used as a fluorescent blue stain for DNA.[1] Hoechst 33258, a monocation species at neutral pH, is made up of three rigid planar moieties, namely, one phenol and two benzimidazole groups (Figure 1),[2] and provides an efficient fluorometric alternative, more sensitive than UV absorbance methods, to quantify nucleic acids.

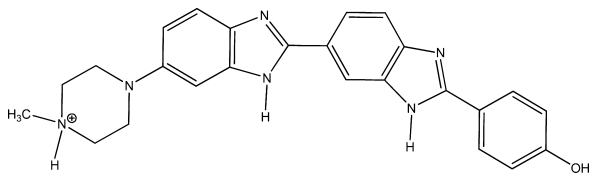

Figure 1. Hoechst 33258, 2′-(4-hydroxyphenyl)-5-(4-methyl-1-piperazinyl)-2, 5′-bi-1H-benzimidazole.

The biological interest of Hoechst 33258 is associated with formation of dsDNA complexes. The Hoechst/DNA system has been well studied and a broad consensus exists about the minor groove nature of the DNA binding to Hoechst at low dye concentrations.[3−6] The number of DNA units linked to Hoechst 33258 depends on the DNA/dye ratio.[7] Hoechst 33258 can interact with DNA, but the binding mode depends on the polynucleotide sequence. Thus, Hoechst interacts with AT sequences by minor groove binding, with poly[d(G-C)$_2$] partial intercalation and major groove binding with involvement of dimers has been reported[8−11] and with poly(dG-dC)·poly(dG-dC) it can react in the monomer, dimer and, presumably, tetramer forms.[12]

The propensity of planar dyes to react with nucleic acids, also as aggregates, appears to be quite a general feature. Recent kinetic works have unveiled that both the free metal and the metal bound to porphyrins are able to intercalate into natural DNA, both in the monomer and the dimer forms.[13,14] Also, some mechanistic studies of the interaction of thioflavin-T with ctDNA have shown that this probe (monomer and dimer) can penetrate into the polynucleotide pockets.[15] Regarding Hoechst, Fornarder et al.[8] have concluded that the binding of dimeric Hoechst to A4T4 oligomer is not cooperative and that the molecules are sitting with a small separation apart (one after the other), not in a sandwich structure as proposed earlier.

Likewise, condensation of DNA can normally be achieved by multivalent minor groove ligands. Aggregation of the dye results in a polyvalent, hydrophobic environment responsible for the DNA condensation, significantly affecting the optical features of the system, the physicochemical parameters of the dye, and its interaction with DNA as well.[16,17] Condensation of DNA upon interaction with monovalent Hoechst has been verified by Silva et al. also by analyzing the apparent contour length of the complexes formed;[10] these authors found that the morphological changes of the DNA structure depend on the Hoechst concentration and came to the conclusion that the dye can interact with DNA through two modes of binding, namely, noncooperative and strongly cooperative binding. The maximum extension of the DNA/Hoechst complexes decreases with the ligand concentration, denoting condensation of DNA by the ligand through the observed cooperative process. Since,

Received: December 10, 2014
Revised: March 4, 2015
Published: March 11, 2015

DOI: 10.1021/jp512306c
J. Phys. Chem. B 2015, 119, 4575−4581

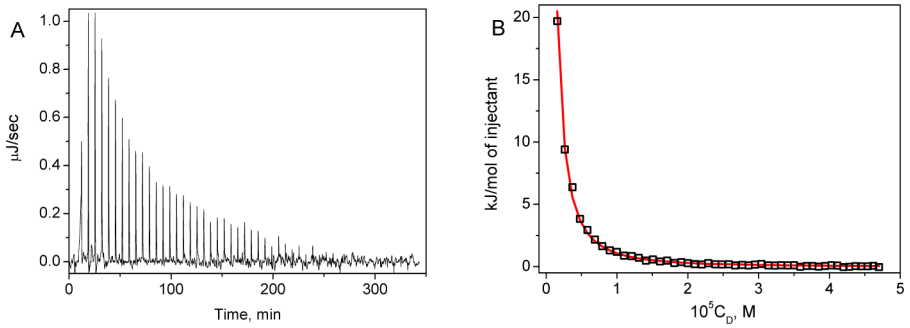

Figure 2. ITC profile for the titration of Hoechst 33258, pH = 7.0, I = 0.10 M (NaCl), and T = 25 °C. (A) Raw data recorded from the sequential injection of the dye into the buffer solution. (B) Integrated heat data versus Hoechst 33258 concentration. The data points reflect the experimental readings to which the dimer dissociation model was fitted; the solid line represents the best fitting curve.

in general, a single monovalent bound ligand is insufficient to cause DNA condensation, such an effect must be related to bound clusters of ligand units.[18] In addition, a strong hydrophobic interaction between DNA and Hoechst can also contribute to the condensation process, as suggested by Saito et al.,[5] who demonstrated that condensation of DNA by Hoechst is independent of the sequence selectivity and the type of binding.

Although self-aggregation of Hoechst 33258 has been reported to involve a stepwise mechanism driven by stacking interactions, so far dimerization has not been observed because the high drug concentration needed favors the formation of higher-order aggregates.[19,20] The divalent groove binder DAPI induces a specific aggregation pattern; this probe causes the DNA double strand to bend, adopting a compact U-shape configuration stabilized by the dye, thus acting as a bridge between the faced segments of the double strand.[21]

In line with earlier contributions on drug-nucleic acid interactions,[22−24] we have conducted a thorough investigation on the behavior of this dye in aqueous solution. We report the self-association of Hoechst 33258 by isothermal titration calorimetry (ITC), absorbance and fluorescence titrations in the presence of different salts, fluorescence quenching measurements, differential scanning calorimetry (DSC), and T-jump relaxation kinetic experiments. The thermodynamic parameters obtained and the mechanistic profile put forward for the aggregation phenomena both provide valuable information that help one understand the overall process and contribute to interpret reliably the mechanism of binding of this dye to DNA.

MATERIALS AND METHODS

Materials. Hoechst 33258 (purity >98%) was from Sigma-Aldrich. Stock solutions, prepared by dissolving weighed amounts of the reagent in water, were kept in the dark at 4 °C. The analytical molar concentration of Hoechst 33258 is denoted as C_D. All the solutions were prepared using deionized water from a Millipore Q apparatus (APS, Los Angeles, California). The ionic strength was adjusted with sodium chloride, NaCl. Sodium cacodylate, $(CH_3)_2AsO_2Na$, was used to maintain the acidity at pH = 7.0.

Methods. pH measurements were performed with a Metrohm 16 DMS Titrino pH-meter, fitted out with a combined glass electrode with a 3 M KCl solution as liquid junction. The ITC experiments were performed at 25 °C with a Nano ITC (TA Instruments, Newcastle, USA). The samples were degassed prior to titration. The stirring speed was maintained constant at 250 rpm. In the course of the titration, the drug was injected into the calorimetric cell (187 μL golden capillary) containing the buffer solution. The data-pairs were treated with a model equation for dimer dissociation using the Nano Analyze Software v2.3.6 (TA Instruments, Newcastle, USA). The thermal behavior of Hoechst 33258 solutions with different concentrations was also monitored by DSC measurements, employing a Nano DSC Instrument (TA, Waters LLC, New Castle, USA). To reduce to a minimum the formation of bubbles upon heating, reference and sample solutions were previously degassed in a degassing station (TA, Waters LLC, New Castle, USA). The samples were scanned from 20 to 90 °C at 3 atm constant pressure and 1 °C min^{-1} scan rate.

The fluorescence titrations were carried out at λ_{exc} = 345 nm and λ_{em} = 498 nm with a Shimadzu Corporation RF-5301PC spectrofluorometer (Duisburg, Germany). The titrations were performed by adding increasing amounts of the salt (or dye, depending on the particular experiment) directly into the cell containing the drug solution. The fluorescence intensity was corrected for every dye concentration considering the inner-filter effect.[25] The spectrophotometric measurements were performed with a HP 8453A diode array spectrophotometer (Agilent Technologies, Palo Alto, CA), fitted out with a computerized temperature control system (±0.1 °C). The concentration data included in the Figures axes were corrected for the dilution effect.

The kinetic experiments were conducted with a T-jump instrument built up according to the Rigler et al. prototype,[26] with the photomultipliers replaced by suitable silica photodiodes (Hamamatsu, S1336, Japan). The instrument, equipped with a lamp−monochromator system as the light source, can work in both the fluorescence and absorbance modes. The kinetic curves were collected with an Agilent 54622A oscilloscope (Santa Clara, CA), transferred to a PC and evaluated with the Table Curve program of the Jandel Scientific package (AISN software, Richmond, CA). The time constants were averaged out to 10 repeated kinetic experiments, the observed spread of time constants being within 10%.

RESULTS AND DISCUSSION

Isothermal Titration Calorimetry. The aggregation of the monocation form of Hoechst 33258 (D) was characterized thermodynamically by ITC experiments performed under physiological conditions, pH = 7.0 and I = 0.10 M (NaCl). The aggregation is described by eq 1:

$$2D \overset{K_D}{\rightleftharpoons} D_2 \quad (1)$$

DOI: 10.1021/jp512306c
J. Phys. Chem. B 2015, 119, 4575−4581

The ITC technique employed has enabled us to determine the thermodynamic aggregation profile by monitoring the reverse process, that is, the dissociation of the aggregated drug in buffered solutions, the heat of dilution gradually decreasing after each drug injection (Figure 2). The dimer dissociation model applied nicely fitted the integration peaks of the binding isotherm. Table 1 lists the fitting parameters. Flat aromatic molecules do aggregate across stacks, the stacking being caused by a variety of interactions: hydrophobic, dipole−dipole and $\pi-\pi$ interactions, dispersion forces and other types of interaction. Previous investigations, mainly on nucleobase-nucleobase self-aggregation, have shown that hydrophobic interactions play an important role in the stacking.

Table 1. Thermodynamic Parameters from Eq 1: Equilibrium Constant (K_D), Enthalpy (ΔH_D) and Entropy (ΔS_D) for Dye Dimerization

10^{-4} K_D, M^{-1}	ΔH_D, kJ mol^{-1}	$-T\Delta S_D$, kJ mol^{-1}
2.4 ± 0.3[a]	−102 ± 4	77 ± 2
3.0 ± 0.3[b]		
3.9 ± 0.9[c]		

[a]ITC. [b]spectrofluorometry. [c]spectrophotometry. pH = 7.0, I = 0.10 M (NaCl), and T = 25°C.

The exothermic aggregation process evolved with entropy decrease, the enthalpy term prevailing at 25 °C; ΔH_0 and ΔS_0 adopt negative values (Table 1), as occurs with self-aggregation of N6, N9-dimethyladenine investigated by osmometry (ΔH_0 = (−36.4) kJ mol^{-1} and $T\Delta S_0$ = (−27 kJ mol^{-1}))[27] and for aggregation of Coralyne (ΔH_0 = −44.7 kJ mol^{-1} and $T\Delta S_0$ = −22.2 kJ mol^{-1}).[22] In agreement with these data, the negative values ΔH_0 and ΔS_0 obtained are explained in terms of surface solute−solvent interactions, which can evolve during the occurrence of stacking.

Effect of NaCl on the Fluorescence and Absorbance of Hoechst 33258. The electrostatic theory applied to eq 1 envisages an increase in the dimer form when the ionic strength is raised. Hence, the enhanced fluorescence recorded upon stepwise addition of NaCl to drug solutions should reflect the formation of increasing amounts of the dimer inherent to the ionic strength effect (Figure 3A). The resulting upward curve reached a plateau for I = 0.08 M and above, evincing the higher fluorescence intensity displayed by the dimer compared to the monomer.

The dimerization constant, defined as $K_D = [D_2]/[D]^2$, depends on the activity coefficients of the monomer (f_D) and dimer (f_{D2}) according to eq 2,

$$K_D = K_D^0 \frac{f_D^2}{f_{D_2}} \tag{2}$$

where K_D^0 represents the thermodynamic aggregation constant at zero ionic strength. Thus, the measured data-pairs (Figure 3B) were analyzed in terms of eq 3:

$$\frac{C_D}{\Delta F} = \frac{1}{\Delta\varphi} + \frac{2K_D^0}{\Delta\varphi^2}\cdot\Delta F\frac{f_D^2}{f_{D_2}} \tag{3}$$

which has been obtained introducing the mass conservation equation for the dye and eq 2 in the relationship $F = \varphi_D[D] + \varphi_{D2}[D2]$. In eq3, C_D represents the overall drug concentration, ΔF and $\Delta\varphi$ are defined as $\Delta F = F - (\varphi_{D2}/2)C_D$ and $\Delta\varphi = (\varphi_D - \varphi_{D2}/2)$, respectively, the f_D^2/f_{D2} ratio being a function of the ionic strength according to eq 4:

$$\frac{f_D^2}{f_{D_2}} = 10^{1.02\cdot F(I)} \tag{4}$$

the $F(I)$ factor being evaluated as

$$F(I) = \frac{\sqrt{I}}{1+\sqrt{I}} \tag{5}$$

Combination of the values for the slope $(2.1 \pm 0.2) \times 10^{-12}$ and intercept $(2.4 \pm 0.1) \times 10^{-8}$ obtained from Figure 3B yielded the dimerization equilibrium constant K^0_D at I = 0 M. Conversion of K^0_D to K_D (I = 0.10 M) by means of the Güntelberg approximation ($\log(fi) = -0{,}5z_i^2(I^{1/2}/(1 + I^{1/2}))$) leads to the value reported in Table 1. Bearing in mind the limits of the electrostatic theory, K_D can be considered in good agreement with the value deduced from the ITC titrations.

Sodium iodide is an efficient quencher of the Hoechst 33258 fluorescence (see below), thereby formation of the dimer could not be observed upon replacement of NaCl by NaI from fluorescence titrations similar to that of Figure 3. To overcome this trouble, two absorbance titrations of Hoechst 33258 were conducted with NaCl and NaI. The isosbestic points at 369 nm for the two sets of spectra recorded up to C_{NaX} = 0.10 M (Figure 4A collects the spectra with NaI) unveil the formation of the D_2 dimer from the D monomer, in the presence of the two salts.

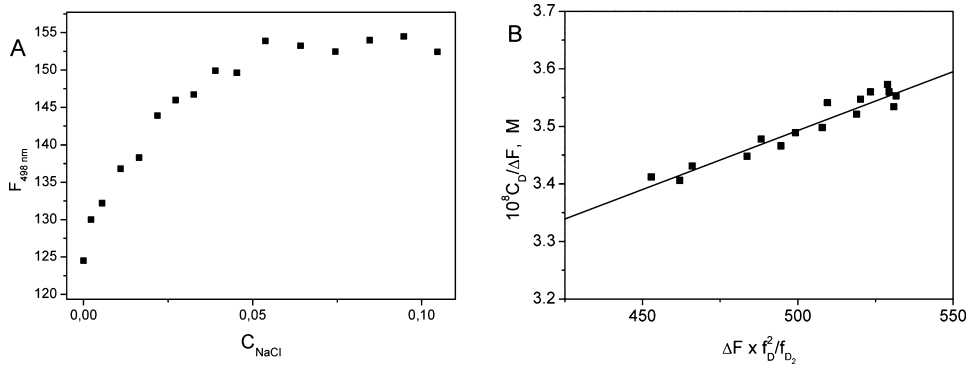

Figure 3. (A) Fluorescence titration of Hoechst 33258 with 2 M NaCl. $C°_D = 9.5 \times 10^{-6}$ M, λ_{exc} = 345 nm, λ_{em} = 498 nm, pH = 7.0 and T = 25 °C. The fluorescence intensity was corrected by the dilution factor. (B) Relevant analysis according to eq 3.

DOI: 10.1021/jp512306c
J. Phys. Chem. B 2015, 119, 4575−4581

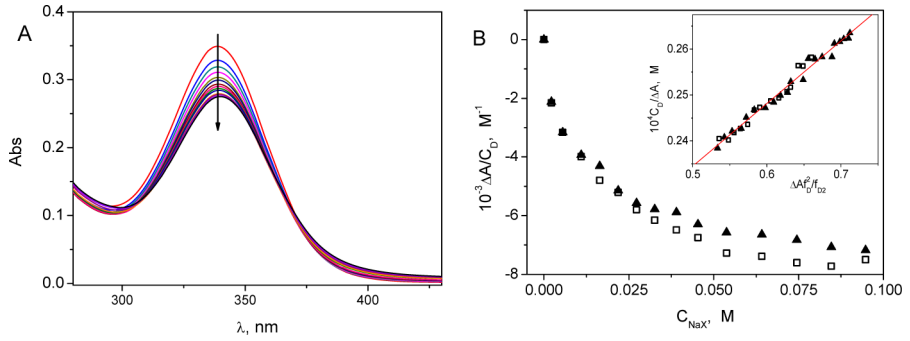

Figure 4. (A) Evolution of the absorbance spectra of Hoechst 33258 upon addition of increasing amounts of NaI; (B) isothermal titration with NaCl (▲) and NaI (□) at 340 nm. $C_D = 9.5 \times 10^{-6}$ M, pH = 7.0, and $T = 25$ °C. Inset: fitting of data according to eq 3.

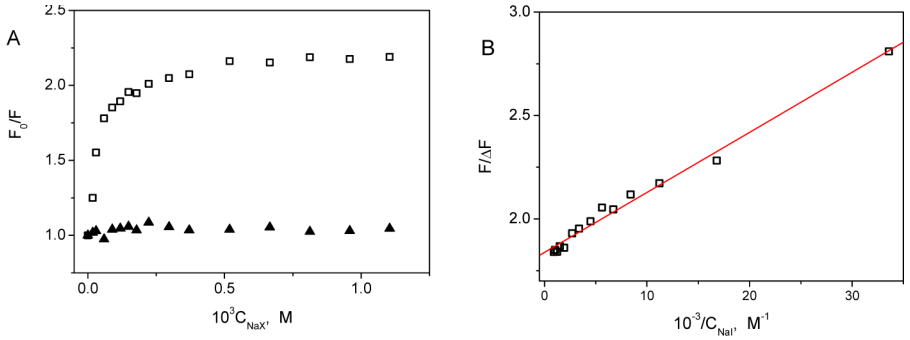

Figure 5. Stern–Volmer plots for (▲) Hoechst 33258/NaCl and (□) Hoechst 33258/NaI systems. (A) Relevant analysis of Hoechst 33258/NaI according to eq 6; (B). $C_D = 1.3 \times 10^{-5}$ M, pH = 7.0, I = 0.10 M ($NaClO_4$), $\lambda_{exc} = 345$ nm, $\lambda_{em} = 498$ nm, and $T = 25$ °C.

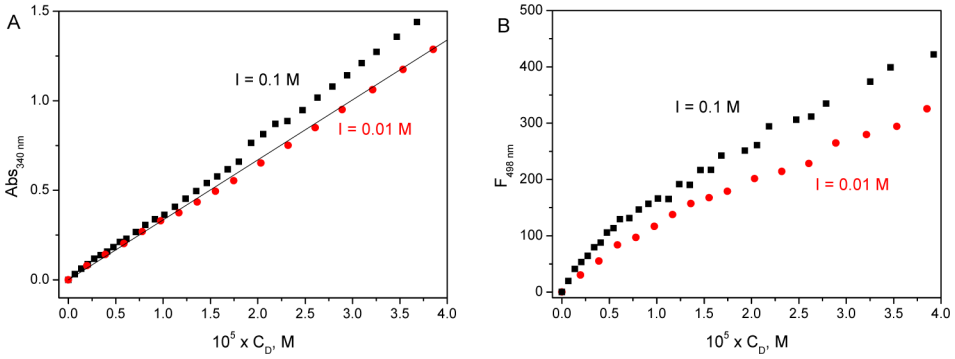

Figure 6. (A) Absorbance and (B) fluorescence spectra recorded for Hoechst 33258 in buffered solutions (●) I = 0.01 M (NaCl) and (■) I = 0.10 M (NaCl). $C_D = (0–4) \times 10^{-5}$ M, $\lambda_{exc} = 345$ nm, $\lambda_{em} = 498$ nm, pH = 7.0 and $T = 25$ °C.

The resulting monophasic isotherm enlightens the decrease in absorbance at 340 nm as the ionic strength was increased (Figure 4B). The absorbance data of the titration curves were analyzed according to eq 3 by a similar approach, taking into account that $\Delta F = \Delta A$ and $\Delta\varphi = \Delta\varepsilon$. The same straight line function has served to fit the data-pairs for the two systems, NaCl and NaI (Figure 4B, inset), indicating that the ionic strength utilized plays a main role in the aggregation, with no significant difference regarding the type of salt used. The dimerization constant K^0_D obtained for $I = 0$ M was recalculated for $I = 0.10$ M, yielding the K_D value reported in Table 1. The K_D values obtained were an order of magnitude higher than that reported by Buurma and Haq under the same acidity and ionic strength conditions,[20] but their values were obtained employing Hoechst 33258 in the 2.2 to 10.0 mM concentration range, much larger than the concentrations utilized in the experiments of Figures 2–4. Therefore, the dimerization model could not be applied; a stepwise aggregation model was feasible, instead.

The effect of the ionic strength on the aggregation might be one of the main reasons for the lack of consensus regarding the second type of binding Hoechst/DNA, somehow related to Hoechst aggregation. The interaction of DNA with Hoechst dimers at high concentration has not been explained in detail hitherto; in fact, general consensus as to the second complex formed is lacking so far. For example, Fornarder et al.[8] have concluded that the binding of Hoechst dimers to A4T4 oligomer is noncooperative, while Silva et al.[10] have reported that condensation of the DNA–Hoechst complexes is cooperative. The formation of dimers under high dye concentration conditions and their interaction with the groove of DNA has been suggested recently by our group.[15] Therefore, the interaction of DNA with Hoechst dimers is feasible.[8,10,16–19]

DOI: 10.1021/jp512306c
J. Phys. Chem. B 2015, 119, 4575–4581

Quenching Effect. The quenching effect was observed at constant ionic strength (I = 0.1 M, $NaClO_4$), recording the fluorescence spectra upon addition to Hoechst 33258 solutions of increasing amounts of NaI (or NaCl). Figure 5 shows the efficient quenching of the fluorescence of Hoechst 33258 by NaI, while in the presence of NaCl the fluorescence remained essentially unaltered under the same conditions. The Stern–Volmer plot for NaI shows nonlinear trend (Figure 5A). The downward curvature could be analyzed by the modified Stern–Volmer model, eq 6:[25]

$$\frac{F}{\Delta F} = \frac{1}{f_a} + \frac{1}{f_a K_a [Q]} \quad (6)$$

where $\Delta F = F_0 - F$, f_a is the fraction of the initial fluorescence accessible to the quencher, $[Q]$ is the quencher (NaI) concentration, and K_a is the Stern–Volmer quenching constant of the accessible fraction. From Figure 5B, it follows that $K_a = (5.3 \pm 0.1) \times 10^4$ M^{-1} and $f_a = 0.55 \pm 0.04$; the latter value reveals that (roughly) half the dye molecules are accessible to the quencher, suggesting that, for I = 0.10 M and 1×10^{-5} M dye concentration, Hoechst 33258 adopts the dimer form.

Influence of Hoechst concentration on the absorbance and fluorescence effects. The formation of fluorescent dimers, depending on the ionic strength and the dye concentration, has also been evinced by monitoring the variation of the absorbance and fluorescence intensity as a function of the Hoechst 33258 concentration upon stepwise addition of increasing amounts of the dye to a buffer solution at two different ionic strengths.

Figure 6A shows the absorbance behavior at 0.01 and 0.10 M ionic strength (NaCl). For I = 0.01 M, deviation from Lambert–Beer law was not observed over the full concentration range of the dye, whereas formation of dimers could be responsible for the deviation observed for I = 0.10 M. On the other side, the observed fluorescence intensity for I = 0.10 M (NaCl) was higher than for I = 0.01 M (NaCl) (Figure 6B). The two types of experiments performed demonstrate that the dimer species, present at 0.10 M (NaCl), is more fluorescent than the monomer, even at low dye concentration, thus bearing out the behavior shown in Figure 3.

Differential Scanning Calorimetry. DSC experiments were conducted at pH = 7.0 and I = 0.10 M employing dye concentration 10–100 times higher than in the spectrophotometric experiments (Figure 7). The effect of the dye concentration on the melting temperature unveils that different extents of aggregation are at work.[20] Figure 7 reveals the formation of multimers higher than dimers. For the lowest concentration used (10^{-4} M), two transitions were observed at 65.4 and 79.5 °C, the former being ascribable to decomposition of aggregates higher than dimers; the latter, most probably stemming from the dimer–monomer transition, was not clearly observable when the concentration experienced a 10-fold increase. This notwithstanding, the shoulder at 72 °C of the smoother band could correspond to a dimer–monomer transition, indicating that, under such conditions, the dimer form prevails even at higher temperature.

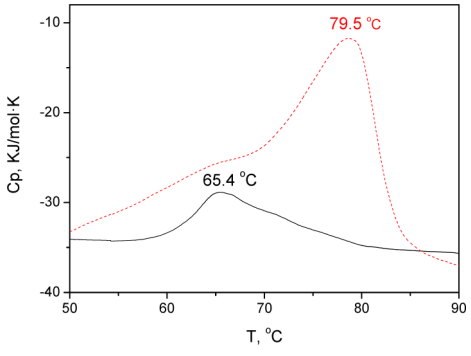

Figure 7. DSC curves of Hoechst 33258 solutions. (—) $C_D = 1 \times 10^{-3}$ M, (– –) $C_D = 1 \times 10^{-4}$ M, scan rate 1 °C/min, pH = 7.0 and I = 0.10 M (NaCl).

UV–Vis Melting Experiments. The change in absorbance with temperature was observed also under different ionic strength conditions (I = 0.025, 0.10, and 0.50 M NaCl). Figure 8 shows the different behaviors observed, concurrent with different types of aggregates; however, as the temperature was raised, the trends tended to merge, reflecting the aggregates formed coming toward common, simpler dimer/monomer equilibrium.

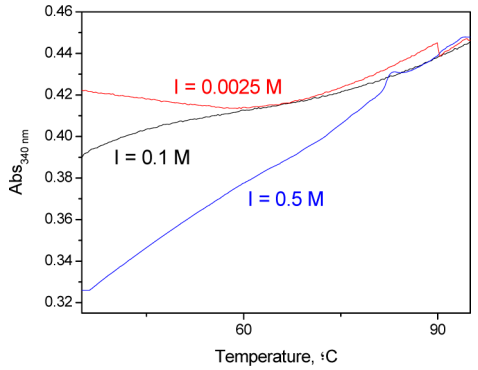

Figure 8. Evolution of the absorbance of Hoechst 33258 with temperature at different ionic strengths. $C_D = 1.0 \times 10^{-4}$ M, pH = 7.0, λ = 340 nm, and T = 25 °C. Experiments performed with 0.1 cm pathlength cells.

Chemical Relaxation. The self-aggregation process was investigated also by a relaxation kinetic approach. T-jump experiments were performed at 0.50 M NaCl and different dye concentrations, yielding single exponential relaxation curves (Figure 9A).

The reciprocal relaxation times, $1/\tau$, obtained from fitting of the single exponential kinetic function to the data-pairs, were independent of the drug concentration (Figure 9B); such constancy of $1/\tau$ should be related to the isomerization of an aggregated form according to eq 7, with $1/\tau = k_f + k_d = (450 \pm 15)$ s^{-1}:

$$D_m \underset{k_d}{\overset{k_f}{\rightleftarrows}} D_m' \quad (7)$$

A deeper kinetic study of the aggregation process was experimentally unfeasible for lower salt content (where the dimer/monomer equilibrium governs) due to the unfavorable signal-to-noise ratio. However, for I = 0.10 M the $1/\tau$ constant was the order of 10^4 s^{-1} (not shown), concurrent with the order of magnitude of time constants measured for dimerization reactions of drugs.[22,28,29]

The 2 orders of magnitude smaller deduced for $1/\tau$ at I = 0.50 M and its insensitiveness to changes in concentration reasonably suggest the occurrence of a monomolecular process that can be identified with eq 7. As to the isomerization of the

DOI: 10.1021/jp512306c
J. Phys. Chem. B 2015, 119, 4575–4581

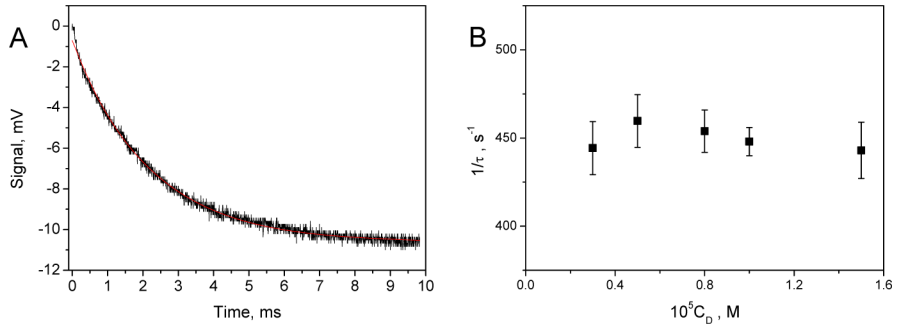

Figure 9. (A) Single exponential relaxation curves obtained for Hoechst 33258 ($C_D = 8.0 \times 10^{-6}$ M). (B) Dependence of the reciprocal relaxation time, $1/\tau$, on the dye concentration. I = 0.50 M (NaCl), pH = 7.0, T = 25 °C.

multimer species, an in-depth description of the structural features of these species lies beyond the scope of this work.

Two types of aggregates were differentiated by their electronic absorption properties compared to the absorption peak of the monomer. For H-aggregates, the units align along face-to-face arrangements, while for J-aggregates the alignment is edge-to-edge. The H-aggregates display broad, blue-shifted absorption peaks compared to the monomer, while highly fluorescent J-aggregates are characterized by sharp, red-shifted absorption spectra.[30] From the experiments of Figure 8, we have compared the absorption spectra at 35° and 95 °C for the different ionic strengths utilized and found that the monomer band at 260 nm (95 °C) shifted to red upon decreasing the temperature, where the dimer ratio increases. Thus, $\Delta\lambda = \lambda(95\ °C) - \lambda(35\ °C)$ = 1.0, 3.0, and 4.5 nm for I = 0.0025, 0.10, and 0.50 M, respectively, which would correspond to formation of J-aggregates; as expected in view of the different proportion of aggregate at 35 °C, the extent of shift varied with the ionic strength. However, qualitative tests on geometry optimization, performed by means of the Hyperchem software show that, for Hoechst 33258, H-type aggregation with high surface superimposition is favored. Taking for granted that the isomerization process involves two species with different planar overlapping residues, many different orientations could be considered for the two monomers in the aggregate species. Taking into account the different Hoechst conformers described by Dickerson[31] and Wang[32] in Hoechst–DNA systems, it is clear that the inherent flexibility of the Hoechst molecule in solution due to the free rotation degree between the benzimidazoles, benzimidazole–piperazine, and benzimidazole–phenol rings supports the existence of isomers for multimer species. It has been found that the dye aggregation may consist of different steps, where the transformation from one to the other occurs via slow kinetic processes.[33]

CONCLUSION

In conclusion, Hoechst 33258 can form dimers and multimers, even at very low concentration, depending on the ionic strength. The dimer species, more fluorescent than the monomer, explains the excellent behavior of this dye as a fluorescent probe. Under physiological conditions, only micromolar concentrations can ensure reasonably high amounts of the monomer in solution.

AUTHOR INFORMATION

Corresponding Author

*E-mail: begar@ubu.es; Tel: +34 947 258819.

Notes

The authors declare no competing financial interest.

ACKNOWLEDGMENTS

The financial support by Obra Social "la Caixa", project OSLC-2012-007 and Junta de Castilla y León (Fondo Social Europeo), project BU-299A12-1, Spain, are gratefully acknowledged.

REFERENCES

(1) Latt, S. A.; Stetten, G. J. Spectral Studies on 33258 Hoechst and Related Bisbenzimidazole Dyes Useful for Fluorescent Detection of Deoxyribonucleic Acid Synthesis. *J. Histochem. Cytochem.* **1976**, *40*, 24–33.

(2) Ladinig, M.; Leupin, W.; Meuwly, M.; Respondek, M.; Wirz, J.; Zoete, V. Protonation Equilibria of Hoechst 33258 in Aqueous Solution. *Helv. Chim. Acta* **2005**, *88*, 53–67.

(3) Neidle, S. DNA Minor-Groove Recognition by Small Molecules. *Nat. Prod. Rep.* **2001**, *18*, 291–309.

(4) Rodger, A.; Norden, B. DNA Structural Features Responsible for Sequence-Dependent Binding Geometries of Hoechst 33258. *Biopolymers* **1996**, *38*, 593–606.

(5) Saito, M.; Kobayashi, M.; Iwabuchi, S.; Morita, Y.; Takamura, Y.; Tamiya, E. DNA Condensation Monitoring After Interaction with Hoechst 33258 by Atomic Force Microscopy and Fluorescence Spectroscopy. *J. Biochem.* **2004**, *136*, 813–823.

(6) Bailly, C.; Colson, P.; Henichart, J.; Houssier, C. The Different Binding Modes of Hoechst 33258 to DNA Studied by Electric Linear Dichroism. *Nucleic Acids Res.* **1993**, *21*, 3705–3709.

(7) Kobayashi, M.; Kusakawa, T.; Saito, M.; Kaji, S.; Oomura, M.; Iwabuchi, S.; Morita, Y.; Hasana, Q.; Tamiya, E. Electrochemical DNA Quantification Based on Aggregation Induced by Hoechst 33258. *Electrochem. Commun.* **2004**, *6*, 337–343.

(8) Fornander, L. H.; Wu, L.; Billeter, M.; Lincoln, P.; Nordén, B. Minor-Groove Binding Drugs: Where Is the Second Hoechst 33258 Molecule? *J. Phys. Chem. B* **2013**, *117*, 5820–5830 (and references therein).

(9) Bailly, C.; Colson, P.; Hénichart, J. P.; Houssier, C. The Different Binding Modes of Hoechst 33258 to DNA Studied by Electric Linear Dichroism. *Nucleic Acids Res.* **1993**, *21*, 3705–3709.

(10) Silva, E. F.; Ramos, E. B.; Rocha, M. S. DNA Interaction with Hoechst 33258: Stretching Experiments Decouple the Different Binding Modes. *J. Phys. Chem. B* **2013**, *117*, 7292–7296.

(11) Moon, J. H.; Kim, S. K.; Sehlstedt, U.; Rodger, A.; Nordén, B. DNA Structural Features Responsible for Sequence-Dependent Binding Geometries of Hoechst 33258. *Biopolymers* **1996**, *38*, 593–606.

(12) Streltsov, S. A.; Zhuze, A. L. Hoechst 33258-Poly(dG-dC)·poly(dG-dC) Complexes of Three Types. *J. Biomol. Struct. Dyn.* **2008**, *26*, 99–113.

(13) Lee, C.; Gong, L.; Shon, Y.; Lee, Y. S.; Lee, S. J.; Han, S.; Kim, S. K. Bis-Intercalation of a cationic porphyrin dimer linked with

DOI: 10.1021/jp512306c
J. Phys. Chem. B 2015, 119, 4575–4581

trietylene glycol derivative to DNA from the major groove. *J. Porphyrins Phthalocyanines* **2012**, *16*, 1159−1166.
(14) Gong, L.; Lee, C.; Kim, G.; Lee, Y. S.; Lee, S. J.; Kim, S. K. Consecutive Intercalation of a Cationic Porphyrin Dimer Between the GC Base-Pairs: A Kinetic Study. *J. Porphyrins Phthalocyanines* **2012**, *16*, 1303−1307.
(15) Biancardi, A.; Biver, T.; Burgalassi, A.; Mattonai, M.; Secco, F.; Venturini, M. Mechanistic Aspects of Thioflavin-T Self-Aggregation and DNA Binding: Evidence for Dimer Attack on DNA Grooves. *Phys. Chem. Chem. Phys.* **2014**, *16*, 20061−20072.
(16) Kaushik, M.; Kukreti, S. Temperature Induced Hyperchromism Exhibited by Hoechst 33258: Evidence of Drug Aggregation from UV-Melting Method. *Spectrochim. Acta, Part A* **2003**, *59*, 3123−3129.
(17) Loontiens, F. G.; Regenfuss, P.; Zechel, A.; Dumortier, L.; Clegg, R. M. Binding Characteristics of Hoechst 33258 with Calf Thymus DNA, poly[d(A-T)] and d(CCGGAATTCCGG): Multiplestoichiometries and Determination of Tight Binding with a Wide Spectrum of Site Affinities. *Biochemistry* **1990**, *29*, 9029−9039.
(18) Bloomfield, V. A. DNA Condensation by Multivalent Cations. *Biopolymers* **1997**, *44*, 269−282.
(19) Sarkar, R.; Pal, S. K. Interaction of Hoechst 33258 and Ethidium with Histone1-DNA Condensates. *Biomacromolecules* **2007**, *8*, 3332−3339.
(20) Buurma, N. J.; Haq, I. Calorimetric and spectroscopic studies of Hoechst 33258: Self-association and binding to non-cognate DNA. *J. Mol. Biol.* **2008**, *381*, 607−621.
(21) Beccia, M. R.; Biver, T.; Pardini, A.; Secco, F.; Venturini, M.; Busto, N.; Lopez-Cornejo, M. P.; Martin-Herrera, V. I.; Prado-Gotor, R. The Fluorophore 4′,6-Diamidino-2-Phenylindole (DAPI) Induces DNA Folding in Long Double-Stranded DNA. *Chem.—Asian J.* **2012**, *7*, 1803−1810.
(22) Garcia, B.; Ibeas, S.; Ruiz, R.; Leal, J. M.; Biver, T.; Boggioni, A.; Secco, F.; Venturini, M. Solvent Effects on the Thermodynamics and Kinetics of Coralyne Self-Aggregation. *J. Phys. Chem. B* **2009**, *113*, 188−196.
(23) Biver, T.; Boggioni, A.; García, B.; Leal, J. M.; Ruiz, R.; Secco, F.; Venturini, M. New Aspects of the Interaction of the Antibiotic Coralyne with RNA: Coralyne Induces Triple Helix Formation in Poly(rA)·Poly(rU). *Nucleic Acids Res.* **2010**, *38*, 1697−1710.
(24) Hoyuelos, F. J.; Garcia, B.; Leal, J. M.; Busto, N.; Biver, T.; Secco, F.; Venturini, M. RNA Triplex-to-Duplex and Duplex-to-Triplex Conversion Induced by Coralyne. *Phys. Chem. Chem. Phys.* **2014**, *16*, 6012−6018.
(25) Lakowicz, J. R. *Principles of Fluorescence Spectroscopy*, 4th ed.; Springer: New York, 2006; p 56.
(26) Rigler, R.; Rabl, C. R.; Jovin, T. M. A Temperature-Jump Apparatus for Fluorescence Measurements. *Rev. Sci. Instrum.* **1974**, *45*, 580−588.
(27) Pörschke, D.; Eggers, F. Thermodynamics and Kinetics of Base-Stacking Interactions. *Eur. J. Biochem.* **1972**, *26*, 490−498.
(28) Biver, T.; Boggioni, A.; Secco, F.; Turriani, E.; Venturini, M.; Yarmoluk, S. Influence of Cyanine Dye Structure on Self-Aggregation and Interaction with Nucleic Acids: A Kinetic Approach to TO and BO Binding. *Arch. Biochem. Biophys.* **2007**, *465*, 90−100.
(29) Biver, T.; De Biasi, A.; Secco, F.; Venturini, M.; Yarmoluk, S. Cyanine Dyes as Intercalating Agents: Kinetic and Thermodynamic Studies on the DNA/Cyan40 and DNA/CCyan2 Systems. *Biophys. J.* **2005**, *89*, 374−383.
(30) Mooi, S. M.; Heyne, B. Size Does Matter: How To Control Organization of Organic Dyes in Aqueous Environment Using Specific Ion Effects. *Langmuir* **2012**, *28*, 16524−16530.
(31) Pjura, P. E.; Grzeskowik, K.; Dickerson, R. E. Binding of Hoechst 33258 to the Minor Groove of B-DNA. *J. Mol. Biol.* **1987**, *197*, 257−271.
(32) Teng, M. K.; Usman, N.; Frederick, C. A.; Wang, A. H. J. The Molecular Structure of the Complex of Hoechst 33258 and the DNA Dodecamer d(CGCGAATTCGCG). *Nucleic Acids Res.* **1988**, *16*, 2671−2690.
(33) Giovannetti, R.; Alibabaei, L.; Pucciarelli, F. Kinetic Model for Astaxanthin Aggregation in Water−Methanol Mixtures. *Spectrochim. Acta, Part A* **2009**, *73*, 157−162.

DOI: 10.1021/jp512306c
J. Phys. Chem. B 2015, 119, 4575−4581